THE JOURNAL OF BIOLOGICAL CHEMISTRY VOL. 282, NO. 35, pp. 25475–25486, August 31, 2007
Printed in the U.S.A.

Anaerobic Acclimation in *Chlamydomonas reinhardtii*

ANOXIC GENE EXPRESSION, HYDROGENASE INDUCTION, AND METABOLIC PATHWAYS[*][S]

Received for publication, February 16, 2007, and in revised form, April 13, 2007 Published, JBC Papers in Press, June 12, 2007, DOI 10.1074/jbc.M701415200

Florence Mus[‡1], **Alexandra Dubini**[§¶1], **Michael Seibert**[§1], **Matthew C. Posewitz**[§¶1], **and Arthur R. Grossman**[‡1,2]

From the [‡]*Department of Plant Biology, Carnegie Institution, Stanford, California 94305,* [§]*National Renewable Energy Laboratory, Golden, Colorado 80401, and* [¶]*Colorado School of Mines, Environmental Science and Engineering Division, Golden, Colorado 80401*

Both prokaryotic and eukaryotic photosynthetic microbes experience conditions of anoxia, especially during the night when photosynthetic activity ceases. In *Chlamydomonas reinhardtii*, dark anoxia is characterized by the activation of an extensive set of fermentation pathways that act in concert to provide cellular energy, while limiting the accumulation of potentially toxic fermentative products. Metabolite analyses, quantitative PCR, and high density *Chlamydomonas* DNA microarrays were used to monitor changes in metabolite accumulation and gene expression during acclimation of the cells to anoxia. Elevated levels of transcripts encoding proteins associated with the production of H_2, organic acids, and ethanol were observed in congruence with the accumulation of fermentation products. The levels of over 500 transcripts increased significantly during acclimation of the cells to anoxic conditions. Among these were transcripts encoding transcription/translation regulators, prolyl hydroxylases, hybrid cluster proteins, proteases, transhydrogenase, catalase, and several putative proteins of unknown function. Overall, this study uses metabolite, genomic, and transcriptome data to provide genome-wide insights into the regulation of the complex metabolic networks utilized by *Chlamydomonas* under the anaerobic conditions associated with H_2 production.

The unicellular green alga *Chlamydomonas reinhardtii* has emerged as a prototype organism for investigating processes such as photosynthesis, nutrient deprivation, flagellar function, and H_2 production (1–12). Although most studies of *Chlamydomonas* have been performed under oxic conditions, it is becoming increasingly apparent that photosynthetic microorganisms frequently experience periods of anoxia. In the laboratory, *Chlamydomonas* cultures may be grown with limited aeration, in low nutrient medium or under low light conditions. Under such conditions, respiratory O_2 uptake may exceed the production of O_2 by photosynthesis leading to the onset of anoxia (9, 13, 14). In the natural environment many photosynthetic microorganisms are also exposed to anoxic conditions. For example, *in situ* studies have demonstrated that cyanobacteria in Octopus Springs at Yellowstone National Park experience anaerobiosis during the night, which triggers a switch from respiratory metabolism and photosynthesis during the day to fermentation metabolism and nitrogen fixation during the night (15).

Based on the draft genome sequence and available literature (16, 17), it is clear that *Chlamydomonas* contains genes encoding proteins that participate in a diverse set of metabolic pathways. Interestingly, *Chlamydomonas* contains several genes encoding proteins usually associated with strict anaerobes, including two [FeFe]-hydrogenase enzymes (18, 19) and the corresponding [FeFe]-hydrogenase maturation proteins (20, 21). Moreover, *Chlamydomonas* is a rare example of a eukaryote that has homologs to all four predominant enzymes used in the fermentative metabolism of pyruvate. These include pyruvate formate lyase (PFL1), pyruvate ferredoxin oxidoreductase (PFR1, often designated as PFOR in other organisms), lactate dehydrogenase, and pyruvate decarboxylase (PDC1). Genes encoding subunits of a pyruvate dehydrogenase complex are also present in the genome and presumably function in the aerobic metabolism of pyruvate.

The *Chlamydomonas* genome is ~120 Mb (http://genome.jgi-psf.org/Chlre3/Chlre3.home.html) and is predicted to contain over 15,000 genes, with a significant number of genes encoding polypeptides involved in anaerobic metabolism (22). A better understanding of anaerobic metabolism in *Chlamydomonas* and metabolic fluxes associated with diurnal periods of light and dark will facilitate the development of physiological models able to predict metabolic fluxes under various environmental conditions. However, at this point relatively little is known regarding the following: (*a*) regulatory mechanisms by which phototrophic microorganisms sense and acclimate to an anoxic environment after periods of photosynthetic activity or to an oxic environment after periods of anoxia; (*b*) the repertoire of genes and proteins required during anaerobiosis and how changes in gene expression link to changing cellular metabolism; and (*c*) changes in metabolite fluxes and the importance of these fluxes in sustaining cell viability during anaerobiosis.

In the laboratory, fermentation pathways become active in *Chlamydomonas* as the environment becomes anaerobic. This is achieved in the dark by sparging cultures with an inert gas (or exogenous reductant) to purge them of O_2 (23–26) or in the

* This work was supported in part by National Science Foundation Grant MCB 0235878 (to A. R. G.), Air Force Office of Scientific Research Grant FA9550-05-1-0365 (to M. C. P.), and by the National Renewable Energy Laboratory, Laboratory Directed Research and Development Program (to M. S.). The costs of publication of this article were defrayed in part by the payment of page charges. This article must therefore be hereby marked "*advertisement*" in accordance with 18 U.S.C. Section 1734 solely to indicate this fact.

[S] The on-line version of this article (available at http://www.jbc.org) contains supplemental Tables I and II and Fig. 1.

[1] Supported by the Office of Biological and Environmental Research, Office of Science, United States Department of Energy.

[2] To whom correspondence should be addressed. Tel.: 650-325-1521 (Ext. 212); Fax: 650-325-6857; E-mail: arthurg@stanford.edu.

light by depriving illuminated, sealed cultures of sulfate (9, 27–29), which results in attenuated rates of photosynthetic O_2 evolution (30). In the dark, fermentation is coupled to the degradation of starch reserves (23, 31, 32). Formate, acetate, and ethanol are formed as major fermentative products, and H_2 and CO_2 gases are emitted as minor products (23, 31, 32). These products are also formed in the light after exposure to sulfur deprivation (27). The formation of fermentation products is primarily controlled at the level of pyruvate, and the ratios of the fermentative products may change as a consequence of culture conditions and the use of different laboratory strains. The PFL1 enzyme catalyzes the cleavage of pyruvate into formate and acetyl-coenzyme A (acetyl-CoA) (33). The acetyl-CoA generated can be reduced to ethanol via acetaldehyde dehydrogenase and alcohol dehydrogenase activities. Alternatively, the acetyl-CoA can be converted to acetate via phosphate acetyltransferase (PAT)[3] and acetate kinase (ACK), yielding ATP (16, 17). Interestingly, Atteia *et al.* (16) reported that the *Chlamydomonas* genome contains two copies each of the *PAT* and *ACK* genes and suggested that the conversion of acetyl-CoA to acetate likely occurs in both the chloroplast and mitochondrion. It should be noted that the PAT proteins are referred to as phosphotransacetylase in several previous publications, but are annotated as PAT in the current assembly of the *Chlamydomonas* genome.

In *Chlamydomonas*, pyruvate may also be oxidized to acetyl-CoA and CO_2 by PFR1, which was recently identified in the *Chlamydomonas* genome (16, 17). In amitochondriate eukaryotes and anaerobic microbes such as species of *Clostridia*, PFOR reduces ferredoxin, providing electrons for H_2 generation via the catalytic activity of hydrogenase. The accumulation of ethanol and formate and the acidification of the cellular environment by organic acids can be toxic to the cells (34), which requires dynamic responses in cellular metabolism to balance ATP production while limiting the accumulation of toxic metabolites.

Anaerobiosis in *Chlamydomonas* is currently of significant interest as it represents a potential means to generate H_2, a biological source of renewable energy. This potential with respect to energy production has stimulated several studies focused on anaerobic metabolism, and the formation and assimilation of H_2 in algae (32, 35–38). In *Chlamydomonas*, H_2 evolution is catalyzed by two [FeFe]-hydrogenases (HYD1 and HYD2) that are localized in the chloroplast stroma and are coupled to electron donation from ferredoxin (18, 19, 39). The *Chlamydomonas* hydrogenases are typically designated as HYDA1 and HYDA2 with the "A" indicating the catalytic enzyme. However, the HYD1 and HYD2 nomenclature is used here for consistency with current *Chlamydomonas* annotations.

The HYD1 and HYD2 enzymes are O_2-sensitive, and H_2 production is only observed under anaerobic conditions (24, 39–41). Anaerobically maintained *Chlamydomonas* generates H_2 in the light or dark through photosynthetic and fermentative pathways, respectively. Transient H_2 photoproduction is observed after illumination of dark, anaerobically acclimated cells grown in nutrient-replete medium (4, 21, 23, 24, 26, 42). However, H_2 production rates rapidly diminish as the O_2, generated from photosynthesis increases to inhibitory levels. Photosynthesis-dependent generation of volumetric amounts of H_2 by *Chlamydomonas* occurs upon sulfur deprivation (9, 27, 28, 43, 44). This activity can be maintained in the light over a period of several days in batch cultures, whereas H_2 production in chemostats can be sustained for several months (45).

Although previous physiological studies have linked fermentation and photosynthetic electron transport to H_2 production in *Chlamydomonas*, a precise knowledge of the metabolic and regulatory context required for H_2 production will be necessary to understand current limitations in H_2 yields. In this study, we have combined molecular and physiological approaches to examine dark anoxic acclimation of *Chlamydomonas* strain CC-425. The ability to generate H_2 and the accumulation of extracellular fermentation products were monitored during the acclimation of *Chlamydomonas* to anaerobic conditions. The levels of transcripts encoding proteins associated with the various fermentation pathways were monitored in conjunction with the formation of these fermentation products. We also used high density, oligonucleotide (70 mer)-based microarrays to obtain insights into the genome-wide responses initiated by anoxia. Although transcripts from a number of genes associated with fermentation metabolism increased, as expected, there was an unanticipated increase in the levels of several transcripts encoding proteins involved in transcriptional/translational regulation, post-translational modification, and stress responses. Insights obtained from the cellular metabolism and gene expression data are being integrated into a larger systems framework that is focused on understanding the flexibility of whole-cell metabolism under rapidly changing environmental conditions.

EXPERIMENTAL PROCEDURES

Strains and Growth Conditions—C. reinhardtii CC-425 (*cw15, sr-u-60, arg7–8, mt+*) wild-type cells were grown in Tris acetate-phosphate (TAP) medium (pH 7.2) (5), supplemented with 200 mg/liter arginine. Algal cultures were maintained at 25 °C, stirred (105 rpm), and exposed to continuous irradiance of 80 μmol m^{-2} s^{-1} PAR. Cell suspensions contained 16–24 $\mu g \cdot ml^{-1}$ total chlorophyll.

Anaerobic Induction of Liquid Cell Suspensions—Chlamydomonas cultures were grown on TAP medium to ~20 $\mu g \cdot ml^{-1}$ total chlorophyll, centrifuged (500 ml of cells) at 2,500 × *g* for 1 min, and resuspended in one-tenth volume (50 ml) of anaerobic induction buffer (AIB) containing 50 mM potassium phosphate (pH 7.0), and 3 mM $MgCl_2$ (24). Hydrogenase activity was elicited by placing concentrated cells into a vial wrapped with aluminum foil to exclude light. The vial was sealed with a rubber septum, flushed with argon for 15 min, and then incubated anaerobically in the dark at room temperature. For measuring H_2 and O_2 production rates, aliquots of cell cultures were

[3] The abbreviations used are: PAT, phosphate acetyltransferase; HPLC, high pressure liquid chromatography; ROS, reactive oxygen species; ADH, alcohol dehydrogenase; HCP, hybrid cluster protein; HIF, hypoxia-inducible factor; PAT, phosphate acetyltransferase; ACK, acetate kinase; MOPS, 4-morpholinepropanesulfonic acid.

placed in a Clark-type oxygen electrode assay chamber maintained at 25 °C and containing 2.25 ml of de-oxygenated MOPS buffer (50 mM, pH 6.8). The algal suspension was kept in the dark for 2 min, exposed to ~700 μmol m^{-2} s^{-1} of actinic light filtered through a solution of 1% $CuSO_4$ for 3 min, and then returned to the dark for 1.5 min. Clark-type oxygen electrodes were used simultaneously to measure H_2 and O_2 production rates.

Chlorophyll Measurements—Chlorophyll *a* and *b* content was determined spectrophotometrically in 95% ethanol (5).

Metabolite Analysis—Organic acid analysis was performed by liquid chromatography (Hewlett Packard Series 1050 HPLC) using an Aminex HPX-87H (300 × 7.8 mm) ion exchange column. Anaerobically adapted cells were collected at the indicated times and centrifuged, and the supernatant was transferred to a new vial and frozen in liquid N_2 for subsequent analysis. Samples were thawed, centrifuged, and filtered prior to HPLC injection. Twenty μl of cell culture supernatant was injected onto the column and eluted with 8 mM filtered sulfuric acid (J. T. Baker Inc.) at a flow rate of 0.5 ml·min^{-1} at 45 °C. Retention peaks were recorded using Agilent ChemStation software, and quantification was performed by comparisons with known amounts of standards for each of the organic acids.

Ethanol was measured using the YSI 2700 SELECT electrochemical probe (YSI Inc.). This system allows direct reading of ethanol in solution at the enzyme sensor. The enzyme alcohol oxidase, which converts ethanol to acetaldehyde, was immobilized on the enzyme membrane. Identical supernatants were used for metabolite and ethanol analysis; 10 μl of the supernatant was required for the measurement.

Extraction of RNA for Real Time PCR and Microarray Analysis—Total RNA was isolated using the plant RNA reagent protocol, as described by the manufacturer (Invitrogen). Approximately 40 μg of isolated RNA was treated with 5 units of RNase-free DNase (Ambion) for 30 min at room temperature. The Qiagen RNeasy MinElute kit (Qiagen) was used to purify DNase-treated total RNA from degraded DNA, tRNA, 5.5 rRNA, DNase, contaminating proteins, and potential inhibitors of the reverse transcriptase reaction. The A_{260} of the eluted RNA was measured, and 4 μg of purified RNA was reserved to prepare labeled samples for microarray analysis.

Reverse Transcription Reactions—First strand cDNA synthesis was primed from purified, total RNA template using specific primers for each of the *Chlamydomonas* genes of interest (shown as the reverse primers in supplemental Table 1), or with $(dT)_{12-18}$ for the ferredoxin genes (the genes are designated *FDX*, with *PETF* as the exception). The reverse transcription reaction was done using the reverse transcriptase Superscript III kit (Invitrogen), as described by the manufacturer. The specific primers were annealed to 250 ng of total RNA and extended for 1 h at 55 °C using 200 units of reverse transcriptase Superscript III. $(dT)_{12-18}$ primers were annealed to 250 ng of total RNA and extended for 1 h at 50 °C using 200 units of reverse transcriptase Superscript III.

Quantitative Real Time PCR—Levels of specific transcripts in total mRNA from each sample were quantified by real time PCR using the Engine Opticon system (Bio-Rad). Four μl of single-stranded cDNA from the reverse transcriptase reaction (see above) was used as template for the real time PCR experiments. The real time PCR amplifications were performed using reagents from the DyNAmo HS SYBR green real time PCR kit (Finnzymes). Specific primers were designed to amplify gene regions consisting of 100–200 nucleotides. Amplifications were performed using the following cycling parameters: an initial single step at 95 °C for 10 min (denaturation) was followed by 40 cycles of the following: (*a*) 94 °C for 10 s (denaturation), (*b*) 56 °C for 15 s (primer annealing for the *RACK1*, *HYD1*, *HYD2*, *HYDEF*, *HYDG*, *PFL1*, *PFR1*, *PAT1*, *ACK2*, *PETF*, *FDX2*, *FDX3*, *FDX4*, *FDX5*, *FDX6*, *AMYB1*, *AMYB3*, *ADH1*, *CAT1*, ppGpp synthetase/degradase, *TAB2*, *HCP4*, *PDC1*, and *NADTH* genes) or 54 °C for 15 s (primer annealing for the *PAT2*, *ACK1*, and *PFLA* genes), and (*c*) 72 °C for 15 s (elongation). Annotations associated with these genes are described elsewhere in the text and figure legends. A final single step at 72 °C for 10 min followed these 40 cycles. Melting curve analyses were performed on all PCRs to ensure that single DNA species were amplified, and the product sizes were verified by agarose gel electrophoresis. The relative expression ratio of a target gene was calculated based on the $2^{-\Delta\Delta C_T}$ method (46), using the average cycle threshold (C_T) calculated from triplicate measurements. Relative expression ratios from three independent experiments are reported. The *RACK1* gene, previously named *CBLP*, was used as a constitutive control gene for normalization. The primers used for reverse transcription and real time PCR are described in supplemental Table 1 and were designed using Primer3 software.

Microarray Fabrication—Microarrays were fabricated at the Stanford Functional Genomics Facility at Stanford University. Oligonucleotides to be printed were suspended in 8 μl of 3× SSC on a Beckman Coulter BioMek FX liquid handling robot to a concentration of ~50 μM. The print material was deposited onto Corning GAPS II or UltraGAPS slides using a custom-built microarray robot equipped with Majer Precision MicroQuill 2000 array pins. Replicate spots were created by printing the entire plate set twice in succession. The ".gal" file, which reports the specific genes (and gene models when available) and their location on the array as well as gene annotation information, is available on line. Printed slides were maintained in a desiccator. Prior to use, slides were hydrated in a humidity chamber (100% humidity) for 5 min followed by immediate snap drying on a 100 °C hot plate (~3 s, array side up), and the array elements were then UV cross-linked to the aminosilane surface of the slide at 600 mJ using a Stratalinker (Stratagene).

Labeling and Purification of Reverse-transcribed cDNAs—Labeling and purification of reverse-transcribed cDNAs were performed as described previously (47). Four micrograms of purified RNA was adjusted to 4 μl with sterile milliQ-treated water. One microliter of oligo-dT(V) (2 μg·μl^{-1}), consisting of 23 consecutive T residues followed at the 3′ end by an A, T, G, or C, was added to the solution prior to heating the reaction mixture for 10 min at 70 °C and then quickly chilled the mixture on ice. The following reagents were then added to the reaction mixture: 2 μl of 5× superscript buffer; 1 μl of 0.1 M dithiothreitol, 0.2 μl of 50× dNTPs (5 mM dATP, dCTP, dGTP, and 10 mM dTTP), 1 μl of Cy3- or Cy5-dUTP, and 0.8 μl of Superscript III (200 units·μl^{-1}); the final reaction volume was 10 μl. After

allowing the reaction to proceed at 42 °C for 2 h, an additional aliquot of 0.5 μl Superscript III was added, and the reaction was continued for an additional 1 h at 50 °C. The reaction was stopped by the addition of 0.5 μl of 500 mM EDTA and 0.5 μl of 500 mM NaOH, and the solution was incubated at 70 °C for 10 min to degrade RNA. Neutralization of the reaction mixture was achieved by adding 0.5 μl of 500 mM HCl.

The QIAquick PCR purification kit (Qiagen) was used to purify labeled cDNA. Cy3- and Cy5-labeled cDNAs were mixed with 90 μl of DNase-free water and 500 μl of Buffer PB (from kit), and the solution was immediately placed onto a QIAquick column. The column was washed with 750 μl of kit Buffer PE by centrifugation at maximum speed for 1 min, and the flow-through was discarded. The wash procedure was repeated, and the column was centrifuged at maximum speed in an Eppendorf microcentrifuge for 2.5 min to remove the remaining buffer. The column was then transferred to a new 1.5-ml Eppendorf tube, and 50 μl of 1/10 kit Buffer EB (v/v), preheated to 40 °C, were applied to the resin bed. After 1 min of incubation, the column was centrifuged at maximum speed for 4 min to elute the labeled cDNAs. The eluate was then dried in the dark in a SpeedVac (keeping the probe in the dark prevents photobleaching).

Hybridization to the Oligonucleotide Array—Hybridization to the arrays was performed as described previously (47). All solutions used in the prehybridization and hybridization protocols were filtered through 0.2-μm Nalgene Bottle-Top filters and, when possible, autoclaved. Prehybridization was performed immediately before starting the hybridization. The arrays were incubated for 1 h in the pre-warmed prehybridization solution (5× SSC, 25% formamide, 0.1% SDS, 0.1 mg/ml bovine serum albumin) at 42 °C. Following this incubation, the slides were transferred to 0.1× SSC and gently agitated at room temperature for 5 min. The 0.1× SSC wash was repeated, and the slides were then transferred to double distilled H_2O for 30 s and dried by centrifugation at 1,000 rpm for 10 min (Eppendorf Centrifuge 5810R). The dried, labeled cDNA was resuspended in 25 μl of milliQ-treated water followed by the addition of 25 μl of 2× hybridization buffer (6× SSC, 0.2% SDS, 0.4 μg/μl poly(A), 0.4 $\mu g \cdot \mu l^{-1}$ yeast tRNA, 40% formamide), both preheated to 40 °C (preventing precipitation of SDS). Resuspended samples were boiled for 3 min and centrifuged for 2 min in an Eppendorf microcentrifuge at full speed to remove debris, and then 50 μl of the probe solution was placed in the middle of the prehybridized dried array. The solution spreads over the entire surface of the array when a large coverslip (microscope cover glass, 12-544-G22X60-1.5, Fisher) is carefully placed over probe solution on the array surface. Three drops of 10 μl of 3× SSC were placed on the surface of the array (not too close to the position of the coverslip), and then the array was sealed in an air-tight chamber and incubated in a 42 °C water bath for 24 h. To wash the slides following the hybridization, containers with 350 ml of 2× SSC, 0.1% SDS were preheated to 42 °C, and 350 μl of freshly prepared 0.1 M dithiothreitol was added to each just before use. Hybridization chambers were removed from the water bath, and individual slides were immersed in 2× SSC, 0.1% SDS (in one of the containers) until the coverslip moved away from the slides. The slides were then transferred to fresh, preheated 2× SSC, 0.2% SDS, and gently dipped up and down for 5 min. This was followed by 5-min washes in 0.1× SSC, 0.1% SDS and then 0.1× SSC, both at room temperature. Slides were rinsed in 0.01× SSC for 10 s and immediately dried by centrifugation. Detailed and updated versions of the protocols used for RNA labeling, slide prehybridization, hybridization, and washing are available on line.

TABLE 1

Rates of H_2 photoevolution, O_2 photoevolution and dark O_2 consumption (μmol gas mg Chl^{-1} h^{-1}) during acclimation to anoxia

Aliquots of acclimated cells were anaerobically transferred with a gas-tight syringe to an anaerobic cell containing deoxygenated buffer as described under "Experimental Procedures." Samples were illuminated and then returned to darkness. The rates of H_2 and O_2 photoproduction were measured concomitantly with two Clark-type electrodes (one poised to measure H_2, the other O_2). The rates of O_2 consumption were measured in the dark after the illumination period.

Time	Rate of O_2 production (light)	Rate of O_2 consumption (dark)	Rate of H_2 production (light)
h			
0	139.3 ± 21.5	40.1 ± 7.5	0
0.5	41.3 ± 5.5	36 ± 8.3	72.2 ± 12.9
2	37.7 ± 5.8	36.7 ± 7.4	123.3 ± 25.8
4	37.0 ± 9.8	39.6 ± 7.6	135.9 ± 19.9

Scanning, Quantification, and Analysis of the Slides—Microarray slides were scanned for Cy5 and Cy3 fluorescent signals using a GenePix 4000B scanner (Molecular Devices). The images, representing spot intensities from scanned slides, were imported into SpotReader (version 1.3.0.5, Niles Scientific) and quantified. Spot positions were defined according to a predefined microarray layout that was subsequently adjusted by eye to help optimize spot recognition. Spot signals that were distorted by dust, locally high backgrounds, or printing flaws were not included in subsequent analyses. Analyses of the data were performed using GeneSpring 6.1 (Agilent Technologies). Images of the fluorescence at 532 nm for Cy3 and 635 nm for Cy5 were recorded and analyzed from the complete array sets (three biological replicates for the time point 0.5 h, four biological replicates for the time points 2 and 4 h, and three slides per time point for each biological replicate, with two copies of each cDNA per slide). RNA samples used to synthesize the probes that were hybridized to the slides were from independent experiments. Error models were computed based on replicates. Signal ratios were considered to meet threshold criteria if they passed Student's *t* test for significance with a *p* value of ≤0.05.

RESULTS

Hydrogenase activity, photosynthesis, cellular respiration, and organic acid accumulation were all recorded over the period in which the cells were acclimating to anoxic conditions. As presented in Table 1, the maximum rate of photosynthetic O_2 evolution rapidly declines under dark, anaerobic conditions (within 30 min there is a 3–4-fold decline), and the rate of respiration remains approximately constant whereas the rate of H_2 evolution increases; high rates of H_2 production occur between 2 and 4 h following the initiation of anaerobic acclimation. After 24 h under dark, anaerobic conditions, H_2 production by the cells decreases to ~50 μmol of H_2/mg of $chlorophyll^{-1}$ h^{-1} (not shown). These rates of H_2 production were at levels consistent with previous reports (21, 26).

Congruent with elevated H_2 production following exposure

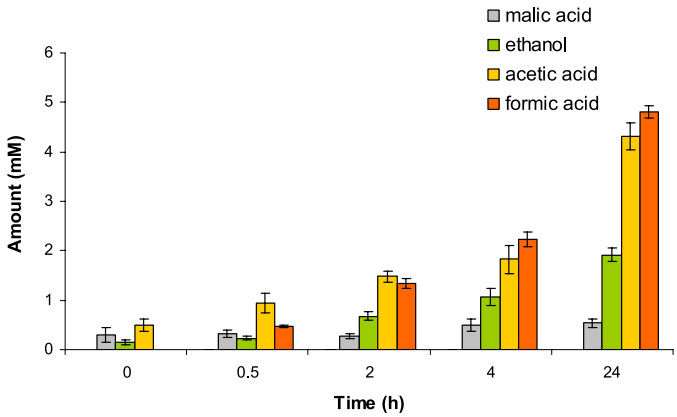

FIGURE 1. **Fermentation products that accumulate in the media of *Chlamydomonas* cultures during acclimation to dark anaerobiosis.** Cells were purged for 30 min with argon in the dark and then kept in the dark for up to 24 h. Samples were taken at the indicated time points (0, 0.5, 2, 4, and 24 h), centrifuged, and filtered, and the medium was analyzed by HPLC. Data are taken from triplicate samples derived from three independent experiments. *Error bars* represent S.D.

of cultures to dark, anaerobic conditions was the accumulation of various fermentation products. As shown in Fig. 1, the fermentative metabolites excreted by *Chlamydomonas* during anoxic acclimation in the dark include malate, formate, acetate, and ethanol; this overall metabolite profile suggests heterofermentation (the accumulation of multiple terminal fermentation products). Formate, acetate, and ethanol are major fermentative products that accumulate in an approximate ratio of 1:1:0.5 after 2 h, whereas malate is a minor product. The ratio of the major fermentation metabolites is similar to that reported by Ohta *et al.* (32) and indicates that both the PFL1 and PFR1 (PFOR) pathways are active when the cells are growing under anaerobic conditions. Moreover, transcripts associated with the PFL1 and PFR1 pathways increase during anoxia, as suggested by real time PCR data (see below). These results indicate a rapid activation of multiple fermentative pathways in cells that are acclimating to anaerobic conditions.

The predominant fermentative pathways used by *Chlamydomonas* as well as the putative locations of the enzymes associated with these pathways are presented in Fig. 2. The putative localization is indicated by specific colors (see Fig. 2 legend), and a question mark indicates that the localization is predicted but not experimentally verified. Starch, the principal carbon-storage compound in this alga, is metabolized to glucose 6-phosphate, which is subsequently oxidized to pyruvate during glycolysis (23). Ohta *et al.* (32) reported a high rate of starch degradation in *Chlamydomonas* upon exposure of the cells to dark, anaerobic conditions; 53% of the total starch was degraded during the first 3 h of the dark incubation. Enzymes necessary for starch degradation, including amylases, have been identified in *Chlamydomonas*. Wanka *et al.* (48) found that amylase activity was undetectable during periods of starch accumulation but was active during net starch breakdown. These results suggest that amylase levels may regulate starch degradation. Accordingly, transcript levels for two β-amylase genes (protein ID 115079, *AMYB1*; JGI *C. reinhardtii* version 3.0) and (protein ID 129211, *AMBY3*; JGI *C. reinhardtii* version 3.0) in *Chlamydomonas* cells exposed to dark anaerobiosis were analyzed by real time PCR. As shown in Fig. 2, both transcript levels increased markedly following anoxic acclimation.

The β-amylases hydrolyze starch into sugars that are enzymatically converted to the central metabolite pyruvate during glycolysis. Conversion of pyruvate into acetyl-CoA is a crucial step in carbon energy metabolism. In many prokaryotes and in some anaerobic eukaryotes, this conversion of pyruvate can occur via either the PFL1 or the PFR1 pathways. *Chlamydomonas* possesses genes encoding both PFL1 (protein ID 146801; JGI *C. reinhardtii* version 3.0) and PFR1 (protein ID 122198; JGI *C. reinhardtii* version 3.0), suggesting that this alga can synthesize acetyl-CoA using both pathways. As shown in Fig. 2, dark anaerobiosis caused a marked increase in both PFL1 and PFR1 mRNA levels. In accordance with the findings of Atteia *et al.* (16), the transcript for the pyruvate formate lyase-activating enzyme (PFLA, also called PFL-AE) (protein ID 194298; JGI *C. reinhardtii* version 3.0) was not significantly influenced by dark anaerobiosis. The acetyl-CoA formed by the actions of PFL1 and/or PFR1 is further metabolized into ethanol by alcohol/aldehyde dehydrogenase (ADH1, also called ADHE) (Protein ID 133318; JGI *Chlamydomonas reinhardtii* v3.0), or into acetate by the sequential actions of PAT1 or PAT2 (Protein IDs 11226 and 191051; JGI *Chlamydomonas reinhardtii* v3.0) and ACK1 or ACK2 (Protein IDs 129982 and 128476; JGI *Chlamydonas reinhardtii* v3.0). An alternative ethanol production pathways involves pyruvate decarboxylase (PDC1, also called PDC) (Protein ID 127786; JGI *Chlamydomonas reinhardtii* v3.0), as shown in Fig. 2*A*. The real time PCR analyses presented in Fig. 2 also demonstrate increased levels of ADH1, PDC1, PAT1, PAT2, ACK1, and ACK2 transcripts following exposure of the cells to dark, anaerobic conditions. In several species of anaerobic microbes, the decarboxylation of pyruvate to acetyl-CoA by PFR1 is linked to H_2 production via the reduction of ferredoxin (49, 50). The levels of transcripts encoding the two *Chlamydomonas* [FeFe]-hydrogenase proteins (HYD1 and HYD2) and the proteins required for maturation of an active [FeFe]-hydrogenase (HYDEF and HYDG), as well as the transcript for PFR1, all increase following exposure of cells to anaerobic conditions (Figs. 2 and 3). The coordination of the abundance of transcripts encoding fermentation proteins is most likely controlled at the level of transcription. Over this same time period, acclimation to dark, anaerobic conditions triggers moderate increases in the levels of transcripts encoding the ferredoxins FDX2 (protein ID 159161; JGI *C. reinhardtii* version 3.0) and FDX5 (protein ID 156833; JGI *C. reinhardtii* version 3.0) but not those encoding four other ferredoxins present on the *Chlamydomonas* genome (Fig. 2).

After establishing that cultures were acclimated to anoxic conditions and correlating changes in metabolite levels with changes in expression of genes associated with fermentation metabolism and hydrogenase activity, microarray (47, 51) analyses were performed to examine the effects of dark anaerobiosis on transcript abundance in a genome-wide context. The relative levels of ~10,000 different transcripts were analyzed following exposure of cells to dark, anaerobic conditions. Total RNA was isolated from cells at 0, 0.5, 2, and 4 h after being transferred from TAP medium to AIB induction buffer under dark, anaerobic conditions (24). Using the oligonucleotide-

based arrays (47), transcript levels at each time point were compared with those of fully illuminated, stirred, and air-saturated CC-425 cells growing in TAP medium (0 h). Transcript levels were filtered to capture those for which there was significant elevation (≥1.5-fold) or diminution (≤0.5-fold) of relative abundance (Table 2 and supplemental Table 2). The *Chlamydomonas* dark anaerobiosis data are available in supplemental Table 3. The transcripts of 514 genes exhibited significant changes of ≥1.5-fold for the three time points following the imposition of dark, anaerobic conditions; this represents somewhat more than 5% of the genes represented on the array. Of the 514 transcripts, 145 encode proteins of known function, 209 encode conserved proteins of unknown function, and 160 encode putative proteins not previously identified. The proteins of known function were placed into functional categories; this information is presented in Table 2 and supplemental Table 2. Furthermore, 46 of the 145 transcripts identified in this study exhibited changes of ≥3.0-fold.

In agreement with the real time PCR data, transcripts encoding several enzymes involved in various aspects of fermentation metabolism increased under dark, anaerobic conditions (Table 2 and supplemental Table 2; Figs. 2 and 3). These include transcripts encoding AMYB1, AMYB3, HYD1, HYD2, HYDEF/G proteins, PDC1, and PFL1. In addition, the abundance of transcripts encoding proteins involved in nitrogen metabolism (glutamate dehydrogenase and hybrid cluster protein (HCP4)) and metabolite balancing (NADH transhydrogenase) also increased. Increased accumulation of glutamate dehydrogenase transcripts is also triggered by low O_2 conditions in *Arabidopsis thaliana* (52, 53).

Not surprisingly, increased levels of transcripts encoding transcription/translation regulatory factors are also observed as cells acclimate to dark anaerobiosis. Some of these

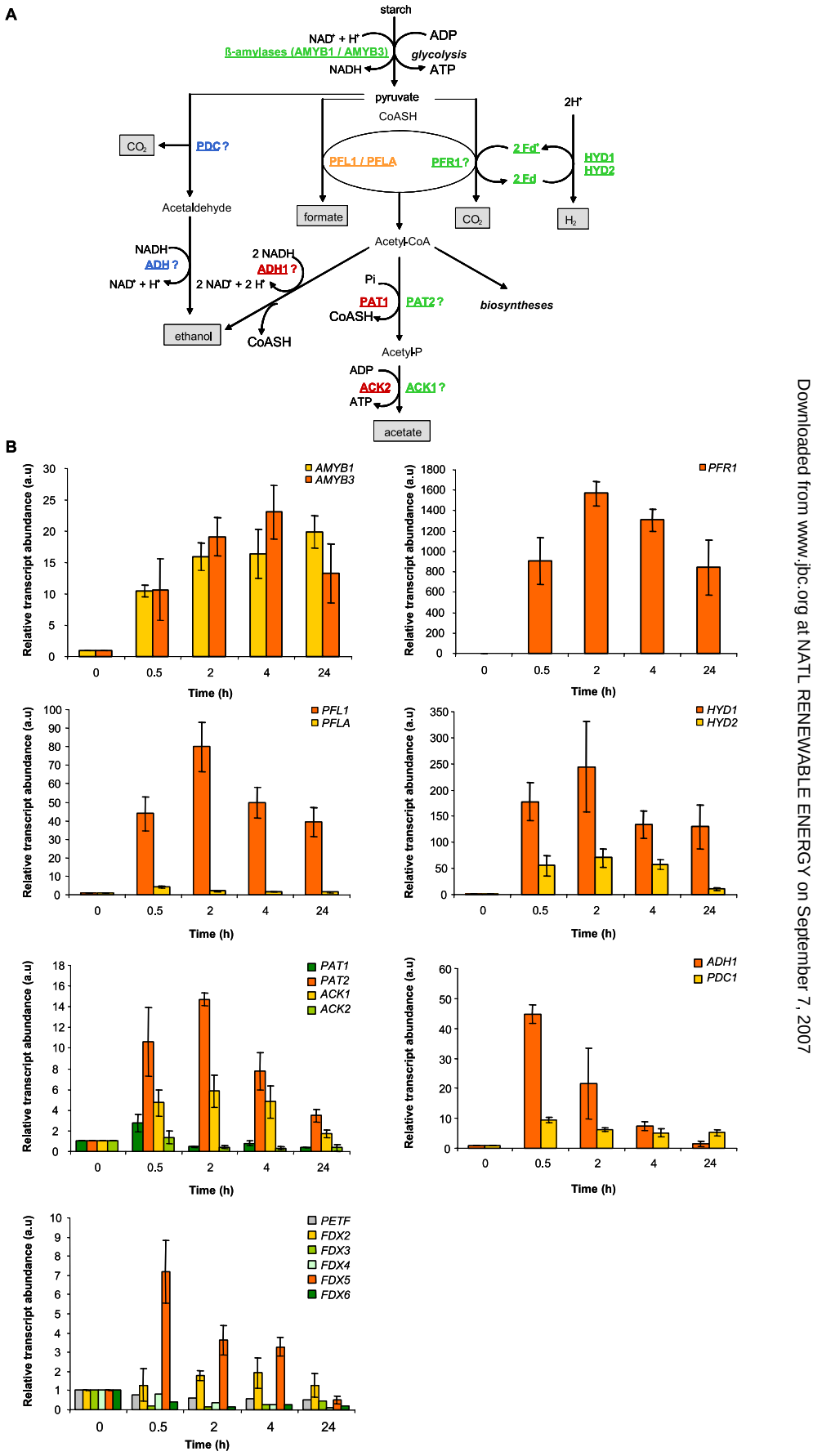

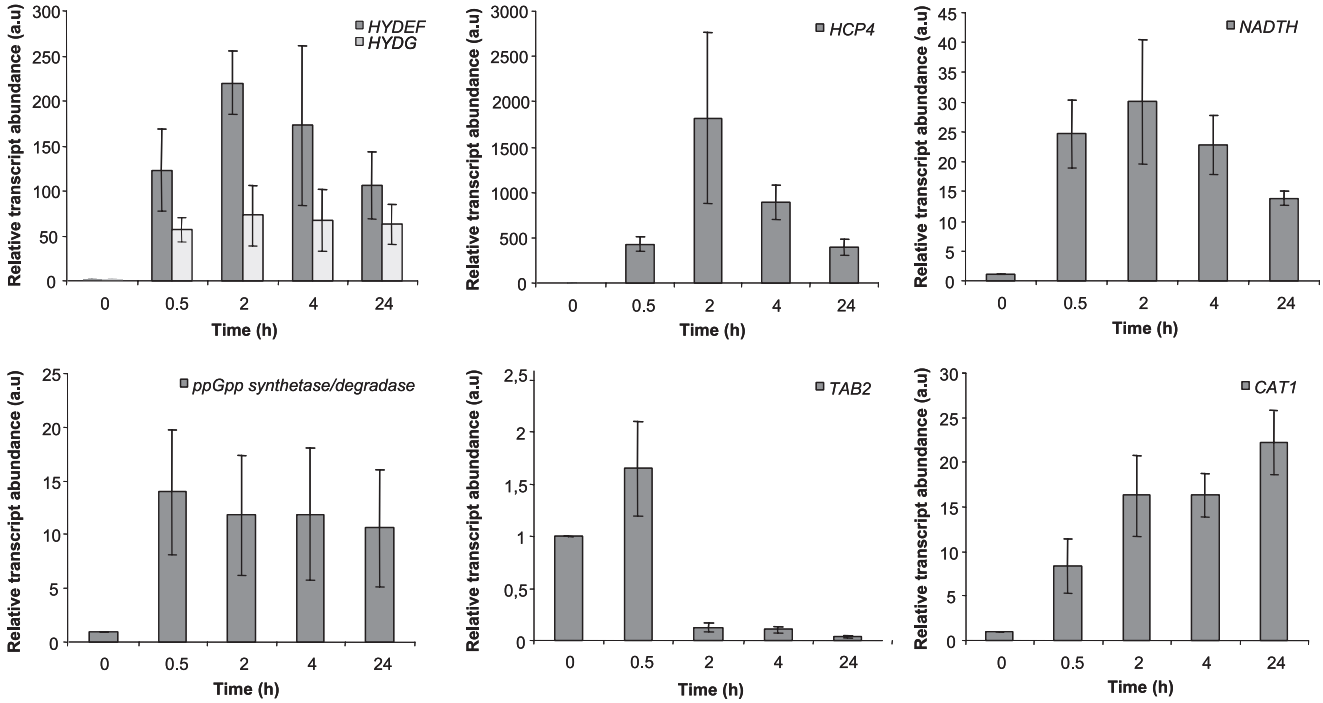

FIGURE 3. **The effect of dark, anaerobic conditions on levels of transcripts encoding *HYDEF*, [FeFe]-hydrogenase maturation protein (protein ID 128256); *HYDG*, [FeFe]-hydrogenase maturation protein (protein ID 196226); *HCP4* (protein ID 148255); *NADTH*, transhydrogenase (protein ID 139758); *ppGpp synthetase/degradase* (protein ID 138526); *TAB2* (protein ID 128415); and *CAT1*, catalase (protein ID 150104).** Total RNA was extracted, and equal amounts of RNA were used for real time PCR. The changes in transcript levels following exposure of the cells to the dark, anaerobic conditions (0.5, 2, 4, and 24 h) are presented as the *n*-fold change (absorbance units, *a.u.*) relative to RNA from time 0 h (just prior to transfer). The results were normalized to *RACK1* transcript levels, which remained constant over the course of the experiment (data not shown). The results show the mean and S.D. (*error bars*) for data from triplicate real time PCR experiments. *a.u.* = arbitrary units.

transcripts encode chloroplast regulatory elements, including the guanosine tetraphosphate synthetase/degradase (ppGpp), and factors that influence the maturation and translation of mRNAs such as EIF5B and TAB2 (Table 2, supplemental Table 2, and Fig. 3). Elevated levels of transcripts for these polypeptides may reflect the need to control translation and post-translation processes that occur in the chloroplast as the cells become anaerobic.

Transcripts encoding several proteases and kinases also increase in *Chlamydomonas* cells following exposure to dark, anaerobic conditions, possibly reflecting the elicitation of specific signal transduction mechanisms, the initiation of specific protease-dependent regulatory processes, and/or the need to redistribute the amino acid resources of the cell.

Paradoxically, the catalase transcript (CAT1) involved in limiting potential damage caused by oxidative stress increases in *Chlamydomonas* cells following the imposition of dark, anaerobic conditions (Table 2 and Fig. 3). Recent evidence suggests that reactive oxygen species (ROS) are involved in anoxic stress responses, and a recent hypothesis suggests that a decrease in O_2 levels and the accumulation of ROS may be recognized by the same cellular sensing mechanism (54). Another intriguing

FIGURE 2. *A,* fermentative metabolism pathways of *Chlamydomonas* during dark anaerobiosis. Starch is accumulated inside the chloroplast during growth in the light and is degraded in the dark. Starch breakdown is greater under anaerobic conditions than under aerobic conditions. In the absence of the complete tricarboxylic acid cycle (during anoxia), acetyl-CoA produced either via the PFL1 or PFR1 pathways enters the acetate-generating PAT-ACK or ADH1 pathways (this occurs in the mitochondria and/or in the chloroplast). PFR1 also has a proposed role in dark, fermentative H_2 production as it reduces ferredoxin, which in turn reduces the hydrogenases (HYD1 and HYD2) catalyzing H_2 production. PFL1 catalyzes the formation of acetyl-CoA and formate from pyruvate. Acetyl-CoA can be further reduced to acetaldehyde and then to ethanol by ADH1 or to acetate by the consecutive actions of PAT1/PAT2 and ACK1/ACK2. Pyruvate can also be decarboxylated to acetaldehyde by pyruvate decarboxylase. The acetaldehyde is subsequently reduced to ethanol, possibly by ADH1 or another ADH that was not identified in this analysis. Proteins on the *Chlamydomonas* genome that are associated with the metabolisms depicted include the following: *AMYB1* and *AMYB3*, β-amylases (protein IDs 115079 and 129211); *PFL1*, pyruvate formate lyase (protein ID 146801); *PFLA*, pyruvate formate-lyase-activating enzyme (protein ID 194298); *PFR1*, pyruvate:ferredoxin oxidoreductase (protein ID 122198); *Fd*, ferredoxin (PETF protein ID 147787; FDX2 protein ID 159161; FDX3 protein ID 196707; FDX4 protein ID 196705; FDX5 protein ID 156833; FDX6 protein ID 196703); *HYD1*, hydrogenase 1 (protein ID 183963); *HYD2*, hydrogenase 2 (protein ID 24189); *PAT*, phosphate acetyltransferase (PAT1 protein ID 11226; PAT2 protein ID 191051); *ACK*, acetate kinase (ACK1 protein ID 129982; ACK2, protein ID 128476); *ADH1*, acetylaldehyde/alcohol dehydrogenase (protein ID 133318); and *PDC1*, pyruvate decarboxylase (protein ID 127786). Known or putative cellular localizations of the proteins depicted are coded by color as follows: *green* for the chloroplast, *red* for the mitochondrion, *orange* for dual chloroplast/mitochondrion localization, and *blue* for the cytoplasm. However, the reader is cautioned that the cellular localizations of ACK1, ADH1 (ADHE), PDC1, ADH, PFR1, and PAT2 have yet to be clearly established experimentally, which is indicated by a "*?*" next to the protein designation. Moreover, dual organelle targeting of some proteins, as observed in the case of PFL1, cannot currently be excluded. *B, bar graphs* show the quantification of the levels of transcripts encoding enzymes critical for fermentation following acclimation to dark, anaerobic conditions (determined using reverse transcriptase and real time PCR). Total RNA was extracted, and equal amounts of RNA were used for the real time PCRs. The changes in transcript levels following exposure of the cells to the dark, anaerobic conditions (0.5, 2, 4, and 24 h) are presented as the *n*-fold change (*a.u.*, absorbance units) relative to RNA from time 0 h (just prior to transfer). The results were normalized to *RACK1* transcript levels, which remained constant over the course of the experiment. The results show the mean and S.D. (*error bars*) for data from triplicate real time PCR experiments. *a.u.* = arbitrary units.

TABLE 2

Transcripts showing ≥3.0-fold change in abundance following exposure of cells to dark, anaerobic conditions

Also shown is the identification number of the deduced protein sequence and the associated annotation.

Oligo ID[a]	Protein model[b]	Scaffold	Annotation	Fold change in transcript abundance[c,d,e]					
				0.5h	t-test	2h	t-test	4h	t-test
			Starch metabolism						
9271.E	115079	scaffold 12	AMYB1 (beta-amylase)	3.76 (n=8/9)	1.50E-03	3.26 (n=9/12)	6.78E-03	3.60 (n=9/12)	2.59E-03
1072.C	129211	scaffold 1	AMYB3 (beta-amylase)	3.92 (n=8/9)	1.12E-05	3.02 (n=9/12)	6.01E-06	2.04 (n=8/12)	7.39E-02
			Metabolism/Fermentation						
9393.E	166317	scaffold 7	putative prolyl 4-hydroxylase	3.03 (n=6/9)	4.76E-03	2.44 (n=8/12)	6.27E-03	3.43 (n=9/12)	1.33E-03
9383.E	148255	scaffold 22	HCP4 (hybrid cluster protein)	4.33 (n=5/9)	2.66E-02	6.41 (n=11/12)	1.63E-05	7.49 (n=11/12)	6.17E-06
8881.D	127786	scaffold 9	PDC1 (pyruvate decarboxylase)	3.63 (n=8/9)	7.99E-04	1.91 (n=9/12)	9.92E-05	1.51 (n=7/12)	5.22E-02
4416.C	79471	scaffold 18	OGD1 (2-oxoglutarate dehydrogenase E1 subunit)	3.12 (n=9/9)	8.65E-04	1.59 (n=6/12)	1.69E-03	1.55 (n=6/12)	6.30E-02
5673.C	190292	scaffold 18	ALA2 (ATPase)	7.49 (n=9/9)	1.46E-03	2.41 (n=9/12)	2.68E-04	2.44 (n=10/12)	1.75E-05
9674.E	59303	scaffold 46	SIR1 (ferredoxin-sulphite reductase)	4.45 (n=8/9)	1.24E-06	2.15 (n=7/12)	6.05E-03	2.09 (n=8/12)	3.79E-02
9898.E	82916	scaffold 76	GDH2 (glutamate dehydrogenase)	6.03 (n=9/9)	3.51E-05	8.24 (n=12/12)	4.40E-06	7.74 (n=10/12)	3.55E-04
9635.E	114525	scaffold 10	putative prolyl 4-hydroxylase	3.89 (n=6/9)	3.90E-04	2.29 (n=10/12)	3.22E-05	2.25 (n=9/12)	3.40E-05
359.A	183963	scaffold 19	HYD1 (chloroplast iron-hydrogenase)	1.76 (n=4/9)	1.05E-01	3.26 (n=12/12)	1.65E-06	3.29 (n=10/12)	7.76E-05
132.A	196226	scaffold 12	HYDG (hydrogenase maturation factor)	4.96 (n=9/9)	3.90E-04	1.78 (n=9/12)	1.41E-03	1.74 (n=7/12)	9.21E-03
8455.D	138637	scaffold 32	ATO1 (acetyl-CoA acyltransferase)	5.11 (n=9/9)	8.77E-06	3.16 (n=9/12)	1.80E-03	3.55 (n=8/12)	1.05E-04
9503.E	139758	scaffold 51	NADTH (NAD(P) transhydrogenase mitochondrial)	3.08 (n=6/9)	5.61E-04	4.89 (n=12/12)	1.43E-07	6.03 (n=11/12)	4.37E-05
			Transcription/Translation/Regulatory elements						
4887.C	141272	scaffold 7	putative translation initiation factor 5B	3.12 (n=8/9)	1.71E-03	1.92 (n=9/12)	4.93E-04	2.87 (n=9/12)	4.46E-03
2497.C	148404	scaffold 21	putative histone acetyltransferase	3.15 (n=7/9)	1.10E-02	1.69 (n=6/12)	4.60E-02	2.63 (n=7/12)	4.72E-03
9134.E	129649	scaffold 19	putative Myb transcription factor	4.31 (n=9/9)	6.99E-05	2.81 (n=9/12)	7.92E-03	1.70 (n=5/12)	2.99E-01
1386.C	187360	scaffold 6	putative Zn-finger GATA type protein	1.63 (n=5/9)	1.45E-02	1.88 (n=7/12)	5.72E-02	3.26 (n=8/12)	9.07E-03
9388.E	163170	scaffold 20	putative histone H4	9.93 (n=9/9)	2.59E-04	8.96 (n=12/12)	3.14E-07	5.32 (n=11/12)	2.99E-05
875.C	186849	scaffold 5	putative RNA-binding protein-like	3.20 (n=9/9)	1.37E-03	0.99 (n=7/12)	9.74E-01	1.07 (n=6/12)	7.74E-01
2691.C	97144	scaffold 7	putative methionyl-tRNA synthetase	3.32 (n=9/9)	3.55E-05	2.62 (n=7/12)	2.28E-04	1.81 (n=6/12)	9.65E-02
8566.D	136620	scaffold 1	putative ATP-dependent RNA helicase	3..90 (n=8/9)	1.97E-03	1.96 (n=9/12)	1.23E-04	2.04 (n=8/12)	2.00E-05
5092.C	186432	scaffold 7	RPB2 (putative DNA-directed RNA polymerase II)	3.19 (n=8/9)	3.76E-06	2.90 (n=10/12)	4.94E-05	2.06 (n=8/12)	1.53E-02
7504.C	100020	scaffold 11	HFO35 (histone-H4 like protein)	3.91 (n=8/9)	2.71E-03	3.67 (n=10/12)	1.97E-05	2.11 (n=7/12)	4.12E-02
6604.C	174408	scaffold 28	putative transcription factor	3.19 (n=8/9)	1.59E-03	2.89 (n=8/12)	2.06E-03	2.80 (n=11/12)	1.83E-04
8088.D	150721	scaffold 31	SMC6A protein	3.72 (n=7/9)	5.85E-03	3.71 (n=10/12)	4.98E-06	3.46 (n=8/12)	4.38E-05
8080.D	120057	scaffold 31	MRPL4 (putative ribosomal protein L4)	3.92 (n=9/9)	1.60E-03	2.49 (n=10/12)	7.48E-06	1.67 (n=6/12)	7.23E-02
9911.E	184151	scaffold 22	putative glycine rich RNA-binding protein	1.85 (n=4/9)	6.06E-02	3.33 (n=10/12)	3.15E-06	2.87 (n=9/12)	2.61E-04
223.A	138526	scaffold 34	ppGpp synthetase/degradase (RelA/SpoT)	3.50 (n=8/9)	1.27E-05	2.34 (n=7/12)	1.07E-02	2.57 (n=7/12)	7.23E-02
			Protein proteolysis						
2367.C	189241	scaffold 14	putative peptidase	4.91 (n=9/9)	1.33E-05	1.74 (n=7/12)	4.67E-02	1.76 (n=7/12)	1.34E-01
4349.C	132770	scaffold 68	PEX7 (peroxisomal targeting signal type 2 receptor)	3.44 (n=9/9)	1.08E-05	2.23 (n=8/12)	3.41E-03	1.51 (n=7/12)	1.50E-01
9710.E	147682	scaffold 17	putative serine endopeptidase	4.71 (n=9/9)	3.93E-04	1.95 (n=9/12)	6.42E-03	2.30 (n=8/12)	1.62E-02
6637.C	148833	scaffold 24	putative acyl glycerol lipase	3.71 (n=9/9)	1.73E-06	2.02 (n=9/12)	9.45E-04	1.72 (n=8/9)	1.07E-02
5863.C	178083	scaffold 46	DNAJ10 (DnaJ like protein)	3.91 (n=8/9)	2.35E-06	2.54 (n=10/12)	4.44E-04	1.75 (n=7/12)	3.60E-02
8338.D	168028	scaffold 4	FAP135 (putative peptidase)	4.59 (n=9/9)	4.69E-07	2.16 (n=9/12)	5.85E-04	3.17 (n=9/12)	4.71E-03
8393.D	190701	scaffold 17	putative peptidase M11	4.25 (n=9/9)	9.22E-07	2.02 (n=9/12)	1.26E-03	1.64 (n=7/12)	1.23E-01
2021.C	205791	scaffold 38	putative alkane hydroxylase/fatty acid desaturase	3.20 (n=6/9)	8.21E-03	1.65 (n=5/12)	5.82E-03	1.59 (n=4/12)	1.38E-01
			Signal transduction						
2401.C	180973	scaffold 233	putative histone acetyltransferase	3.46 (n=9/9)	3.52E-04	1.73 (n=5/12)	4.92E-02	1.58 (n=3/12)	3.27E-02
2529.C	191561	scaffold 28	putative adenylate cyclase	3.34 (n=9/12)	3.17E-04	2.21 (n=8/12)	1.25E-03	1.85 (n=7/12)	5.55E-03
7529.D	58843	scaffold 37	MAK (serine/ threonine protein kinase)	6.07 (n=9/9)	7.89E-04	3.67 (n=11/12)	8.75E-05	1.84 (n=7/12)	1.08E-01
3912.C	101787	scaffold 1	putative protein kinase	3.66 (n=9/9)	1.56E-03	1.90 (n=9/12)	2.11E-04	1.55 (n=6/12)	1.07E-01
5731.C	192767	scaffold 36	putative guanylate cyclase	3.08 (n=8/9)	7.78E-05	1.90 (n=7/12)	1.77E-03	1.91 (n=7/12)	4.15E-02
5451.C	59450	scaffold 52	putative protein kinase	5.40 (n=9/9)	1.51E-03	1.61 (n=5/12)	1.06E-01	1.89 (n=8/12)	2.67E-02
6107.C	94151	scaffold 10	putative protein kinase	4.20 (n=9/9)	9.07E-04	2.81 (n=10/12)	2.03E-05	2.62 (n=9/12)	1.31E-02
3892.C	99469	scaffold 9	putative protein kinase	3.12 (n=8/9)	8.65E-04	1.59 (n=6/12)	1.69E-03	1.55 (n=6/12)	6.30E-02
			Stress protein						
103.A	150104	scaffold 30	CAT1 (catalase/peroxidase)	4.72 (n=9/9)	1.83E-08	2.12 (n=9/12)	9.31E-06	1.91 (n=8/12)	1.71E-02

[a] Identification number for the array element.
[b] Identification number of protein model (JGI *C. reinhardtii* v3.0: http://genome.jgi-psf.org/Chlre3/Chlre3.home.html).
[c] Change in transcript abundance at 0.5, 2, and 4 h after transferring cells to dark, anaerobic conditions relative to time 0 h (just prior to transfer).
[d] Average of three biological replicates for the time point 0.5 h and four biological replicates for the time points 2 and 4 h. Three technical repetitions were done for each biological repetition (each slide contained each array element in duplicate). In parentheses, the number of slides on the total number of slides examined for each condition where the transcript is present in a ratio ≥3.0 (3-fold increase; shown in red).
[e] Student's *t* test; grey shading denotes genes examined by real time PCR.

observation is that there are increased levels of transcripts encoding four putative prolyl hydroxylases (protein IDs 166317, 111255, 114525, and 143800) (Table 2 and supplemental Table 2), which require O_2 as a substrate. As described below, these proteins may be serving as O_2 sensors in *Chlamydomonas* that function to modulate protein activity in response to O_2 levels.

The transcripts of 58 genes exhibited significant changes of ≤0.5-fold, for the three time points following the imposition of dark, anaerobic conditions; this represents somewhat more than 0.5% of the genes on the array. Of the 58 transcripts, 10 encode proteins of known function, 20 encode conserved proteins of unknown function, and 28 encode putative proteins not previously identified. The 10 transcripts encoding those proteins for which a function (or putative activity) is known are given in supplemental Table 2 (protein IDs 144352, 10538, 126287, 120881, 143516, 118588, 141584, 141291, 167916, and 153061), whereas the data for all down-regulated transcripts are presented in supplemental Table 3. A number of the genes for which the transcripts decline during anaerobiosis encode proteins that are putatively associated with signal transduction and metabolite transport.

DISCUSSION

Physiological and molecular/genomic techniques were employed to analyze the pathways used by *Chlamydomonas* during acclimation to anaerobic conditions. Although aspects of fermentation in *Chlamydomonas* have been reported (23, 32,

55), these previous studies were performed without the benefit of a nearly complete genome sequence or high density DNA microarrays to probe gene expression (47).

Fermentation and Anaerobic Metabolism—We initially examined fermentative product formation to help guide a detailed characterization of genes differentially expressed following exposure of *Chlamydomonas* to anaerobic conditions. The predominant fermentative products formed were formate, acetate, and ethanol, as described previously (23, 31, 32), and the ratio of products was ~1:1:0.5, respectively, as reported by Ohta *et al.* (32). Product ratios of 2:1:1 have also been reported (23, 31); however, it should be noted that different strains and culturing conditions were used in those studies. The 2:1:1 product ratio would be expected if PFL1 were solely responsible for the conversion of pyruvate to acetyl-CoA. The reduced stoichiometry of formate relative to acetate in the results presented in this study suggests that PFR1, in addition to PFL1, is contributing to the conversion of pyruvate into acetyl-CoA. PFR1 catalyzes the oxidation of pyruvate to acetyl-CoA and CO_2 and the reduction of ferredoxin. The reduced ferredoxin can subsequently be oxidized by a variety of cellular redox proteins, including the [FeFe]-hydrogenases, resulting in the observed production of small amounts of H_2 during fermentation in the dark. Detailed real time PCR analyses demonstrate that the PFR1 transcript increases significantly during anaerobiosis, as do the transcripts for HYD1, HYD2, and the [FeFe]-hydrogenase maturation proteins (HYDEF and HYDG). These data clearly show that expression of genes required for pyruvate oxidation and H_2 production via the PFR1 pathway increase in response to anoxia. Moreover, these data combined with metabolite analyses suggest that significant PFR1 activity occurs concomitantly with PFL1 activity. Genetically engineered disruption of pyruvate metabolism via the PFL1 pathway represents a possible approach to increase yields of dark, fermentative H_2 production in *Chlamydomonas*.

Chlamydomonas appears to contain a single *PFL* gene. However, the PFL1 protein is observed in both the mitochondrion and chloroplast, indicating that this protein is targeted to both organelles (16). The PFL1 protein requires an activating enzyme (PFLA) (56), which is a radical SAM protein containing a [4Fe-4S] cluster. Although the abundance of the *Chlamydomonas PFL1* transcript increases during anoxia, *PFLA* (same as PFL-AE in most organisms) expression remains relatively constant, consistent with a previous report (16). These findings suggest that the PFLA protein is present under aerobic conditions, although *Escherichia coli* PFL-AE activity is O_2-sensitive *in vitro* (56). The *Chlamydomonas* PFLA protein itself would therefore have to undergo an activation process under anaerobic conditions, implying that PFLA is poised to activate PFL1 upon switching from aerobiosis to anaerobiosis, thereby rapidly initiating aspects of fermentation metabolism. Alternatively, the accumulation of the PFLA protein may be controlled at the translational level.

The PFL1 and PFR1 reactions both yield acetyl-CoA, which can be converted to acetate via the PAT/ACK pathway, resulting in ATP production. Two copies of genes encoding the latter proteins are present on the *Chlamydomonas* genome. Recent biochemical studies indicate that PAT1 and ACK2 are present in mitochondria (16), whereas PAT2 and ACK1, encoded by genes adjacent to *HYD2* on the genome, are proposed to be localized in the chloroplast (16). The real time PCR data demonstrate increased levels of *PAT1*, *PAT2*, *ACK1*, and *ACK2* transcripts during anoxia. Therefore, increased transcript abundance is observed for all of the fermentative genes required for the conversion of pyruvate to acetate, formate, CO_2, and H_2.

The formation of ethanol during fermentation in *Chlamydomonas* occurs by the reduction of acetyl-CoA via ADH1 (ADHE), resulting in the oxidation of two molecules of NADH. In agreement with the metabolite data, an increase in the levels of ADH1 mRNA occurs during anoxia. Pyruvate can also be converted to ethanol via PDC1 (the expression of which increases during anoxia) and alcohol dehydrogenase pathways (ADH), resulting in the production of ethanol and the oxidation of one NADH (Fig. 2). *Chlamydomonas* is rare among eukaryotes in having both pathways for the production of ethanol (17). The cellular localization of the proteins responsible for ethanol formation is presently unresolved. It is possible that the proteins required for the conversion of acetyl-CoA to either acetate, which yields ATP, or ethanol, which reoxidizes NADH allowing additional cycles of glycolysis, are present in both mitochondria and chloroplasts. Additional studies to localize fermentation pathways used in *Chlamydomonas* are required to demonstrate whether both mitochondria and chloroplasts are able to metabolize pyruvate into acetate and ethanol. The PFR1 protein has an N-terminal extension that is predicted to serve as a chloroplast targeting peptide by PSORT and TargetP. Although there are no biochemical data to corroborate the predicted PFR1 localization, the enzyme is likely to be in the chloroplast because the hydrogenases are chloroplast proteins (18, 39).

A transcript that exhibits an unexpected increase in abundance as *Chlamydomonas* acclimates to anoxia encodes a putative hybrid cluster protein (HCP4), also referred to as the prismane protein or hydroxylamine reductase. HCP4 transcript levels increase over 1,500-fold in response to anoxia, and *HCP4* is among the most significantly up-regulated genes detected in response to anoxia. Moreover, three other *HCP* transcripts on the *Chlamydomonas* genome increase significantly during acclimation to anoxia as determined by real time PCR (data not shown). The *E. coli* HCP enzyme exhibits hydroxylamine reductase activity, reducing hydroxylamine to ammonia (57). However, the K_m for this reaction at pH 7.5 is 38.9 mM, suggesting an alternative *in vivo* substrate.

HCP proteins from a variety of organisms have been extensively studied by biophysical and structural methods and are proposed to contain a novel [4Fe-2S-2O] metallocluster (58, 59). Two isoforms of the enzyme have been reported, which have homology to carbon monoxide dehydrogenase. The latter is able to reduce CO_2 (60). In addition to the unique [4Fe-2S-2O] cluster, an additional metal-binding motif coordinates either a [2Fe-2S] or a [4Fe-4S] cluster. Strict anaerobes typically have a unique spacing of conserved cysteines in this motif relative to facultative anaerobes, and these proteins have been shown to coordinate a [4Fe-4S] cluster in addition to the hybrid cluster. This motif in HCP4 is most similar to the domain typically observed in strict anaerobes. Although widely examined

at the biophysical level, relatively little is known about the function of HCPs *in vivo*. It is expressed under anaerobic conditions in several organisms and has been tentatively associated with nitrate and nitrite metabolism. However, it should be noted that these proteins have also been proposed to be involved in oxidative stress protection (61).

It is currently difficult to rationalize why *HCP4* is among the most highly up-regulated genes associated with the transfer of *Chlamydomonas* from oxic to anoxic conditions. Hydroxylamine is toxic to a variety of cells. For example, it can extract the tetrameric manganese cluster associated with O_2 evolution in photosystem II, and it is possibly formed as a by-product in the reduction of nitrite by nitrite reductase. However, in these studies the cells were cultured in TAP medium, which contains ammonium and does not contain nitrate or nitrite.

The HCPs may oxidize reduced ferredoxin and therefore compete with hydrogenase for electrons from reduced ferredoxin (62). It should also be noted that a sulfite reductase (protein ID 59303), which can also oxidize reduced ferredoxin, is significantly up-regulated during anaerobiosis (Table 2).

The *Chlamydomonas* genome contains four homologs of HCP (protein IDs 148253, 148898, 191403, and 148255) that are similar to proteins present in *Clostridia*, *Desulfovibrio,* and *Shewanella*, all of which contain [FeFe]-hydrogenases. These organisms can reduce a variety of terminal electron acceptors, including nitrate, sulfate, fumarate, and oxidized metal ions, as well as protons during anaerobic respiration. To further investigate the precise function of HCP in *Chlamydomonas*, we are examining the possibility that these proteins are reducing oxidized nitrogen compounds, or other potential substrates, under our experimental conditions.

We also observed, from the microarray analyses, an unanticipated increase in the abundance of catalase mRNA, which may reflect a need to ameliorate the effects of oxidative stress. The induction of genes involved in free radical scavenging and detoxification of ROS (63) is common to a number of stress conditions (64–66), and Klok *et al.* (52) recently noted that expression of many genes involved in the detoxification of ROS (peroxidases, ascorbate peroxidase, monodehydroascorbate reductase, glutathione reductase, and superoxide dismutase) was affected by low O_2 levels in *A. thaliana* root cultures. In *B. japonicum,* an operon encoding a [NiFe]-hydrogenase is expressed under anaerobic conditions concomitantly with nitrogenase, which is O_2-sensitive. Interestingly, transcription of the hydrogenase operon is controlled by FixK2, which also regulates an operon encoding a terminal oxidase with a high affinity for O_2 that is expressed under O_2-limiting conditions (67). Adaptation to anoxia requires cells to invest substantial amounts of cellular energy in the biosynthesis of O_2-labile proteins. Although strict anaerobic conditions are maintained in the laboratory, in natural settings it is likely that organisms such as *Chlamydomonas* become exposed to low amounts of atmospheric O_2 during dark anaerobiosis. It is therefore conceivable that *Chlamydomonas* and other organisms have evolved mechanisms to protect O_2-sensitive enzymes from low levels of O_2 and ROS by both efficiently scavenging residual O_2 and rapidly eliminating any ROS that does form. Once O_2 becomes abundant during periods of high photosynthetic O_2 evolution, a fully oxygenic metabolism is restored, and the anaerobic proteins are degraded.

Regulatory Processes—Numerous factors involved in translation and post-translational processes are critical in controlling chloroplast biogenesis in *Chlamydomonas*. Studies performed over the past several years have indicated that these factors are important for RNA stability, splicing, and initiation of translation (68, 69). TAB2, for example, is required for the synthesis of the chloroplast-encoded photosystem I reaction center polypeptides, PsaB. It is part of a chloroplast-localized protein complex involved in the initiation of translation of *psaB* mRNA (70). The photosystem I complex acts as a light-driven, plastocyanin-ferredoxin oxidoreductase, and the regulation of this complex is critical for maintaining the proper stoichiometry of linear to cyclic electron flow.

Another mRNA product that increases to high levels during anaerobiosis is ppGpp, which is an effector molecule that accumulates to high levels in bacteria during amino acid starvation, and the accumulation of this molecule correlates with the inhibition of RNA and protein synthesis (71). In *E. coli*, ppGpp is synthesized by a ribosome-associated protein encoded by the *relA* gene (ppGpp synthetase I) and by the product of the *spoT* gene (ppGpp synthetase II). The latter is believed to encode a bifunctional enzyme that has both ppGpp synthetic and degradative activities. The putative *Chlamydomonas* ppGpp synthetase/degradase shows marked homology to the RelA-SpoT family of proteins from plants, being 36% identical to *Nicotiana tabacum* Nt-RSH2 and *Capsicum annum* Ca-RSH, 35% identical to *A. thaliana* At-RSH3, and 29% identical to *Suaeda japonica* Sj-RelA (supplemental Fig. 1).

The ppGpp molecule is considered a global regulator and can reprogram bacterial transcription depending on growth conditions. Interestingly, accumulation of ppGpp positively regulates expression of the alternative σ factor RpoS (72). In *E. coli*, RpoS is required for efficient transcription of many stress-induced genes and is believed to regulate hydrogenase 1 levels. Maximal expression of the *hya* operon, which encodes the proteins needed for the synthesis of active Hyd1, required RpoS and the transcriptional regulators AppY and ArcA (73). At this point, no transcriptional regulators involved in the control of anoxic gene expression/translation have been identified in *Chlamydomonas*. Hence, it will be important to determine whether ppGpp and/or *Chlamydomonas* σ factors, such as the recently characterized RpoD (74), are responsible for coordinating some aspect of anaerobiosis and hydrogenase activity via the transcription/translation of chloroplast genes.

Surprisingly, four prolyl hydroxylases are significantly up-regulated in response to anaerobiosis (protein IDs 166317, 111255, 114525, and 143800). Although proline hydroxylation occurs in algal cell wall proteins (75), it is unlikely that these gene products are involved in protein hydroxylation during anaerobiosis because prolyl hydroxylases require O_2 as a substrate (75, 76). Recently, significant advances have been made in understanding the sensing of hypoxia in mammalian cells (77, 78). The HIF is constitutively expressed, and in the presence of O_2, HIF is hydroxylated at conserved proline residues, which targets HIF for ubiquitin-dependent degradation. In the absence of O_2, HIF hydroxylation ceases, and subsequent HIF

protein accumulation triggers the expression of several target genes in response to hypoxia. An intriguing possibility that we are currently investigating is that prolyl hydroxylases, which use O_2 and 2-oxoglutarate as substrates, are synthesized and poised to recognize a return to aerobic conditions. Targeting of fermentative proteins for destruction through protein hydroxylation may then facilitate the return to aerobic respiration under oxygenated conditions. Glutamate dehydrogenase, which deaminates glutamine to 2-oxoglutarate, is also up-regulated, as are several diverse putative proteases. Although highly speculative at this point, the control of fermentative metabolism via prolyl hydroxylase activity would represent a particularly elegant mechanism to sense O_2 and target proteins involved in fermentation metabolism for destruction as the cell transitions from anaerobiosis to aerobiosis.

Most of the transcripts that decline upon imposition of anaerobic conditions encode conserved proteins of unknown function or putative proteins not previously identified. Only a few transcripts encode proteins of known function, and most of them are associated with regulatory processes (transcription/translation regulatory factors, signal transduction factors, and transport factors).

In both *Chlamydomonas* (this study) and *Arabidopsis* (52, 53, 79), several classes of genes are regulated similarly in response to O_2 limitation. These include transcripts encoding the following: (*a*) fermentative and glycolysis enzymes; (*b*) proteins associated with nitrogen metabolism; (*c*) transcription factors and signal transduction proteins; (*d*) enzymes used in the detoxification of reactive oxygen species; and (*e*) proteins regulating calcium flux and/or requiring calcium for activity. In *Arabidopsis*, calcium mobilization and utilization is proposed to play a significant role in adaptation to hypoxia (80). The *Chlamydomonas* microarray data indicate that several transcripts encoding putative calcium-dependent proteins (*e.g.* protein IDs 146645, 189454, 111945, and 187818) increase during anaerobiosis. Calcium fluxes may therefore play a similarly important role in algal anoxic metabolism. The large number of diverse genes that are differentially regulated in response to O_2 levels in both *Chlamydomonas* and *Arabidopsis* highlights the complex regulatory and metabolic pathways used by oxygenic photosynthetic organisms in response to limited O_2 availability.

Genes of Unknown Function—Another significant observation from the microarray data is that the majority (>70%) of differentially expressed genes encode putative proteins of unknown function. *Chlamydomonas* is a metabolically versatile organism that is able to perform photosynthesis, aerobic respiration, and ameliorate the potentially toxic consequences of photosynthetically generated O_2. It has several genes encoding proteins associated with anaerobic respiration, as well as one of the most extensive sets of fermentative proteins yet observed. It is capable of using diverse anaerobic pathways that are unprecedented in a single organism. Moreover, under conditions of sulfate deprivation in the light, *Chlamydomonas* can balance photosynthesis, aerobic respiration, and fermentation pathways, concomitantly (27). It is likely that a number of the proteins that currently have no known function are involved in the regulation, metabolic partitioning, and/or function of the extraordinary metabolic networks of *Chlamydomonas*.

Summary—Numerous fermentative pathways are available to *Chlamydomonas*, and apparently parallel metabolic processes occur in the mitochondria and the chloroplast. This study, combined with a number of other reports, highlights the metabolic flexibility of *Chlamydomonas*. There is currently significant interest in engineering *Chlamydomonas* for the production of desired metabolites such as H_2, organic acids, and ethanol. In these studies, additional examinations of the proteins involved in acclimation to anoxic conditions and accurate localization of the proteins involved will provide a foundation for metabolic engineering and modeling of the metabolic pathways in *Chlamydomonas*. They will also facilitate a better understanding of the anaerobic metabolic fluxes occurring in *Chlamydomonas*.

Accurate models of overall cellular metabolism will have to account for many physiological processes, as well as consider metabolite fluxes in multiple cellular compartments, the exchange of metabolites between organelles, and NADH transhydrogenase activity. The availability of the *Chlamydomonas* genome sequence, combined with high throughput "omics"-based approaches, will provide the foundation for continuing examination and a more comprehensive understanding of the extraordinary metabolic capabilities of *Chlamydomonas*.

Acknowledgments—Sabeeha Merchant is gratefully acknowledged for the generous gift of ferredoxin primers. We thank J. Shrager for extensive technical support.

REFERENCES

1. Dent, R. M., Haglund, C. M., Chin, B. L., Kobayashi, M. C., and Niyogi, K. K. (2005) *Plant Physiol.* **137,** 545–556
2. Ghirardi, M. L., King, P. W., Posewitz, M. C., Maness, P. C., Fedorov, A., Kim, K., Cohen, J., Schulten, K., and Seibert, M. (2005) *Biochem. Soc. Trans.* **33,** 70–72
3. Ghirardi, M. L., Posewitz, M. C., Maness, P.-C., Dubini, A., Yu, J., and Seibert, M. (2007) *Annu. Rev. Plant Biol.* **58,** 71–91
4. Happe, T., Hemschemeier, A., Winkler, M., and Kaminski, A. (2002) *Trends Plant Sci.* **7,** 246–250
5. Harris, E. H. (1989) *The Chlamydomonas Sourcebook. A Comprehensive Guide to Biology and Laboratory Use*, Academic Press, San Diego
6. Harris, E. H. (2001) *Annu. Rev. Plant Physiol. Plant Mol. Biol.* **52,** 363–406
7. Im, C. S., Zhang, Z., Shrager, J., Chang, C. W., and Grossman, A. R. (2003) *Photosynth. Res.* **75,** 111–125
8. Kruse, O., Rupprecht, J., Bader, K. P., Thomas-Hall, S., Schenk, P. M., Finazzi, G., and Hankamer, B. (2005) *J. Biol. Chem.* **280,** 34170–34177
9. Melis, A., Zhang, L., Forestier, M., Ghirardi, M. L., and Seibert, M. (2000) *Plant Physiol.* **122,** 127–136
10. Moseley, J. L., Chang, C. W., and Grossman, A. R. (2006) *Eukaryot. Cell* **5,** 26–44
11. Rochaix, J. D. (2002) *FEBS Lett.* **529,** 34–38
12. Snell, W. J., Pan, J., and Wang, Q. (2004) *Cell* **117,** 693–697
13. Moseley, J., Quinn, J., Eriksson, M., and Merchant, S. (2000) *EMBO J.* **19,** 2139–2151
14. Quinn, J. M., Eriksson, M., Moseley, J. L., and Merchant, S. (2002) *Plant Physiol.* **128,** 463–471
15. Steunou, A. S., Bhaya, D., Bateson, M. M., Melendrez, M. C., Ward, D. M., Brecht, E., Peters, J. W., Kuhl, M., and Grossman, A. R. (2006) *Proc. Natl. Acad. Sci. U. S. A.* **103,** 2398–2403
16. Atteia, A., van Lis, R., Gelius-Dietrich, G., Adrait, A., Garin, J., Joyard, J., Rolland, N., and Martin, W. (2006) *J. Biol. Chem.* **281,** 9909–9918
17. Hemschemeier, A., and Happe, T. (2005) *Biochem. Soc. Trans* **33,** 39–41
18. Forestier, M., King, P., Zhang, L., Posewitz, M., Schwarzer, S., Happe, T.,

Ghirardi, M. L., and Seibert, M. (2003) *Eur. J. Biochem.* **270,** 2750–2758
19. Happe, T., and Kaminski, A. (2002) *Eur. J. Biochem.* **269,** 1022–1032
20. Posewitz, M. C., King, P. W., Smolinski, S. L., Smith, R. D., Ginley, A. R., Ghirardi, M. L., and Seibert, M. (2005) *Biochem. Soc. Trans.* **33,** 102–104
21. Posewitz, M. C., King, P. W., Smolinski, S. L., Zhang, L., Seibert, M., and Ghirardi, M. L. (2004) *J. Biol. Chem.* **279,** 25711–25720
22. Grossman, A. R., Croft, M., Gladyshev, V. N., Merchant, S. S., Posewitz, M. C., Prochnik, S., and Spalding, M. H. (2007) *Curr. Opin. Plant Biol.* **10,** 190–198
23. Gfeller, R. P., and Gibbs, M. (1984) *Plant Physiol.* **75,** 212–218
24. Ghirardi, M. L. (1997) *Appl. Biochem. Biotechnol.* **63,** 141–151
25. Greenbaum, E. R., Guillard, R. L., and Sunda, W. G. (1983) *Photochem. Photobiol.* **37,** 649–655
26. Posewitz, M. C., Smolinski, S. L., Kanakagiri, S., Melis, A., Seibert, M., and Ghirardi, M. L. (2004) *Plant Cell* **16,** 2151–2163
27. Kosourov, S., Seibert, M., and Ghirardi, M. L. (2003) *Plant Cell Physiol.* **44,** 146–155
28. Kosourov, S., Tsygankov, A., Seibert, M., and Ghirardi, M. L. (2002) *Biotechnol. Bioeng.* **78,** 731–740
29. Zhang, L., Happe, T., and Melis, A. (2002) *Planta* **214,** 552–561
30. Wykoff, D. D., Davies, J. P., Melis, A., and Grossman, A. R. (1998) *Plant Physiol.* **117,** 129–139
31. Kreutzberg, K. (1984) *Physiologia Plantarum* **61,** 87–94
32. Ohta, S., Miyamoto, K., and Miura, Y. (1987) *Plant Physiol.* **83,** 1022–1026
33. Wagner, A. F., Frey, M., Neugebauer, F. A., Schäfer, W., and Knappe, J. (1992) *Proc. Natl. Acad. Sci. U. S. A.* **89,** 996–1000
34. Kennedy, R. A., Rumpho, M. E., and Fox, T. C. (1992) *Plant Physiol.* **100,** 1–6
35. Ben-Amotz, A., and Avron, M. (1972) *Plant Physiol.* **49,** 240–243
36. Kessler, E. (1974) in *Algal Physiology and Biochemistry: Botanical Monograph* (Stewart, W. D. P., ed) Vol. 10, pp. 456–473, Blackwell Scientific, Oxford, UK
37. Klein, U., and Betz, A. (1978) *Plant Physiol.* **61,** 953–956
38. Weaver, P. F., Lien, S., and Seibert, M. (1980) *Solar Energy* **24,** 3–45
39. Happe, T., Mosler, B., and Naber, J. D. (1994) *Eur. J. Biochem.* **222,** 769–774
40. Happe, T., and Naber, J. D. (1993) *Eur. J. Biochem.* **214,** 475–481
41. Roessler, P. G., and Lien, S. (1984) *Plant Physiol.* **76,** 1086–1089
42. Graves, D. A., Tevault, C. V., and Greenbaum, E. (1989) *Photochem. Photobiol.* **50,** 571–576
43. Antal, T. K., Krendeleva, T. E., Laurinavichene, T. V., Makarova, V. V., Ghirardi, M. L., Rubin, A. B., Tsygankov, A. A., and Seibert, M. (2003) *Biochim. Biophys. Acta* **1607,** 153–160
44. Kosourov, S., Makarova, V., Fedorov, A. S., Tsygankov, A., Seibert, M., and Ghirardi, M. L. (2005) *Photosynth. Res.* **85,** 295–305
45. Fedorov, A., Kosourov, S., Ghirardi, M., and Seibert, M. (2005) *Appl. Biochem. Biotechnol.* **121,** 403–412
46. Livak, K. J., and Schmittgen, T. D. (2001) *Methods* (*Amsterdam*) **25,** 402–408
47. Eberhard, S., Jain, M., Im, C. S., Pollock, S., Shrager, J., Lin, Y., Peek, A. S., and Grossman, A. R. (2006) *Curr. Genet* **49,** 106–124
48. Wanka, F., Joosten, H. F., and de Grip, W. J. (1970) *Arch. Microbiol.* **75,** 25–36
49. Müller, M. (1993) *J. Gen. Microbiol.* **139,** 2879–2889
50. Müller, M. (1998) in *Evolutionary Relationships among Protozoa* (Coombs, G. H., Vickerman, K., Sleigh, M. A., and Warren, A., eds) pp. 109–127, Kluwer Academic, Dordrecht, The Netherlands
51. Im, C. S., Eberhard, S., Huang, K., Beck, C. F., and Grossman, A. R. (2006) *Plant J.* **48,** 1–16
52. Klok, E. J., Wilson, I. W., Wilson, D., Chapman, S. C., Ewing, R. M., Somerville, S. C., Peacock, W. J., Dolferus, R., and Dennis, E. S. (2002) *Plant Cell* **14,** 2481–2494
53. Liu, F., Vantoai, T., Moy, L. P., Bock, G., Linford, L. D., and Quackenbush, J. (2005) *Plant Physiol.* **137,** 1115–1129
54. Semenza, G. L. (1999) *Cell* **98,** 281–284
55. Gfeller, R. P., and Gibbs, M. (1985) *Plant Physiol.* **77,** 509–511
56. Buis, J. M., and Broderick, J. B. (2005) *Arch. Biochem. Biophys.* **433,** 288–296
57. Wolfe, M. T., Heo, J., Garavelli, J. S., and Ludden, P. W. (2002) *J. Bacteriol.* **184,** 5898–5902
58. Aragao, D., Macedo, S., Mitchell, E. P., Romao, C. V., Liu, M. Y., Frazao, C., Saraiva, L. M., Xavier, A. V., LeGall, J., van Dongen, W. M., Hagen, W. R., Teixeira, M., Carrondo, M. A., and Lindley, P. (2003) *J. Biol. Inorg. Chem.* **8,** 540–548
59. Macedo, S., Mitchell, E. P., Romao, C. V., Cooper, S. J., Coelho, R., Liu, M. Y., Xavier, A. V., LeGall, J., Bailey, S., Garner, D. C., Hagen, W. R., Teixeira, M., Carrondo, M. A., and Lindley, P. (2002) *J. Biol. Inorg. Chem.* **7,** 514–525
60. Ragsdale, S. W. (2004) *Crit. Rev. Biochem. Mol. Biol.* **39,** 165–195
61. Almeida, C. C., Romao, C. V., Lindley, P. F., Teixeira, M., and Saraiva, L. M. (2006) *J. Biol. Chem.* **281,** 32445–32450
62. Valentine, R. C., and Wolfe, R. S. (1963) *J. Bacteriol.* **85,** 1114–1120
63. Douce, R., and Neuburger, M. (1999) *Curr. Opin. Plant Biol.* **2,** 214–222
64. Reymond, P., Weber, H., Damond, M., and Farmer, E. E. (2000) *Plant Cell* **12,** 707–720
65. Schenk, P. M., Kazan, K., Wilson, I., Anderson, J. P., Richmond, T., Somerville, S. C., and Manners, J. M. (2000) *Proc. Natl. Acad. Sci. U. S. A.* **97,** 11655–11660
66. Seki, M., Narusaka, M., Abe, H., Kasuga, M., Yamaguchi-Shinozaki, K., Carninci, P., Hayashizaki, Y., and Shinozaki, K. (2001) *Plant Cell* **13,** 61–72
67. Vignais, P. M., and Colbeau, A. (2004) *Curr. Issues Mol. Biol.* **6,** 159–188
68. Rochaix, J. D., Perron, K., Dauvillée, D., Laroche, F., Takahashi, Y., and Goldschmidt-Clermont, M. (2004) *Biochem. Soc. Trans.* **32,** 567–570
69. Rochaix, J. D. (2004) *Plant Cell* **16,** 1650–1660
70. Dauvillée, D., Stampacchia, O., Girard-Bascou, J., and Rochaix, J. D. (2003) *EMBO J.* **22,** 6378–6388
71. Tedin, K., and Norel, F. (2001) *J. Bacteriol.* **183,** 6184–6196
72. Eichel, J., Chang, Y. Y., Riesenberg, D., and Cronan, J. E., Jr. (1999) *J. Bacteriol.* **181,** 572–576
73. King, P. W., and Przybyla, A. E. (1999) *J. Bacteriol.* **181,** 5250–5256
74. Bohne, A. V., Irihimovitch, V., Weihe, A., and Stern, D. B. (2006) *Curr. Genet* **49,** 333–340
75. Kaska, D. D., Gunzler, V., Kivirikko, K. I., and Myllyla, R. (1987) *Biochem. J.* **241,** 483–490
76. Hieta, R., and Myllyharju, J. (2002) *J. Biol. Chem.* **277,** 23965–23971
77. Ivan, M., Kondo, K., Yang, H., Kim, W., Valiando, J., Ohh, M., Salic, A., Asara, J. M., Lane, W. S., and Kaelin, W. G., Jr. (2001) *Science* **292,** 464–468
78. McDonough, M. A., Li, V., Flashman, E., Chowdhury, R., Mohr, C., Lienard, B. M., Zondlo, J., Oldham, N. J., Clifton, I. J., Lewis, J., McNeill, L. A., Kurzeja, R. J., Hewitson, K. S., Yang, E., Jordan, S., Syed, R. S., and Schofield, C. J. (2006) *Proc. Natl. Acad. Sci. U. S. A.* **103,** 9814–9819
79. Gonzali, S., Loreti, E., Novi, G., Poggi, A., Alpi, A., and Perata, P. (2005) *Ann. Bot.* (*Lond.*) **96,** 661–668
80. Sedbrook, J. C., Kronebusch, P. J., Borisy, G. G., Trewavas, A. J., and Masson, P. H. (1996) *Plant Physiol.* **111,** 243–257